A Parametric Study of Laser Induced Thin Film Spallation

by Junlan Wang, Richard L. Weaver, Nancy R. Sottos

ABSTRACT—We report parametric studies of elastic wave generation by a pulsed laser and associated spalling of thin surface films by the corresponding high stresses. Two different substrate materials, single crystal Si (100) and fused silica, are considered. Spallation behavior of Al thin films is investigated as a function of substrate thickness, film thickness, laser energy, and various parameters governing the source. Surface displacement due to the stress wave is measured by Michaelson interferometry and used to infer the stresses on the film interface. Consistent with previous studies, the maximum stress in the substrate and at the film/substrate interface increases with increasing laser fluence. For many of the conditions tested, the substrate stress is large enough to damage the Si. Moreover, the maximum interface stress is found to increase with increasing film thickness, but decrease with increasing substrate thickness due to geometric attenuation. Of particular significance is the development of a decompression shock in the fused silica substrates, which results in very high tensile stresses at the interface. This shock enhances the failure of thin film interfaces, especially in thicker samples.

KEY WORDS—Laser spallation, thin film, interface adhesion, stress wave, decompression shock

Introduction

Thin films are crucial components in a wide range of multilayer microelectronic and optical devices. They are also desirable candidates for micro-actuators in micro-electro-mechanical devices. The size scales and dissimilar nature of the constituents present great challenges in regard to thermo-mechanical integrity and reliability.[1] Large residual stresses are induced in films during fabrication, which then have a significant impact on mechanical properties and performance. Under appropriate conditions the residual stress can cause the film to decohere, crack, or buckle away from the substrate. A particular challenge is the design and implementation of test procedures that measure thin film interface properties.

Several practical techniques for the measurement of thin film adhesion have been described in the literature, of which the most common are the scratch, peel, pull, blister, and indentation tests. The first quantitative uses of the scratch test were reported by Heavens[2] and Weaver.[3] Later, this method was used to calculate adhesion energies by Laugier[4] and Hull *et al.*[5] In the scratch test, a conical diamond indenter is driven into a film sample until a load drop occurs, indicating delamination. The scratch test is simple but the data are difficult to interpret.[5] In the peel test, first used by Strong,[6] an adhesive tape is applied directly to the film. A force is applied to the tape and used to peel off the film from the substrate. This test is only suitable for films in which the adhesion to the substrate is weaker than to the tape. For cases where the adhesion is considerably higher, the pull test[5,7] is often used. In a pull test, a stud is attached to the film using a strong adhesive. The perpendicular force required to remove the stud is measured and then divided by the area of removed film to calculate the adhesive strength. A major limitation of the pull test is that the maximum measurable strength cannot exceed the maximum bonding strength of available adhesives. Another technique is the blister test, in which a film layer is deposited on a rigid, flat substrate with a center perforation. A pressurizing fluid is injected through the perforation creating a blister and causing a progressive debonding of the film/substrate interface at a critical pressure.[8,9] Indentation induced delamination has also been proposed for measuring film adhesion.[10,11] During all these tests, scratch, peel, pull, blister and indentation, the interface is subjected to very high stress levels and consequent inhomogeneous deformations. Large amounts of plastic deformation can result (especially in the peel test) and dominate the behavior during the test.[12] The stress fields are difficult to analyze and the resulting adhesion measurements tend to be qualitative and comparative.

A novel laser spallation technique was first introduced by Vossen[13] in which the film is loaded using stress waves produced by short laser pulses as developed by Ready,[14] Anderholm,[15] Peercy,[16] Yang,[17] and Fox.[18] This technique involved impinging a high-energy laser pulse (duration of nanoseconds) from a Q-switched laser (1064 nm wavelength) onto a thin absorbing layer confined between a plate and the back surface of the substrate. Upon absorbing the laser energy, the sudden expansion of the confined layer generated a compressive stress wave directed towards the test film. The reflection of the compressive wave packet from the surface of the test film generated a tensile pulse which led to spallation of the test film. Yang[17] used an x-cut quartz crystal to measure the stress at the front surface of the substrate.

Gupta and co-workers[19,20] further developed Vossen and Yang's technique to measure the thin film interfacial strength. Like Yang,[17] the stress impinging the interface was measured using a micro-electronic device with x-cut piezoelectric crystal. Later,[21–24] a laser Doppler interferometer was

Junlan Wang is a Graduate Student, Richard L. Weaver is a Professor, and Nancy R. Sottos is a Professor, Department of Theoretical and Applied Mechanics, University of Illinois at Urbana-Champaign, Urbana, IL 61801, USA.

Original manuscript submitted: October 9, 2000.
Final manuscript received: September 10, 2001.

introduced to measure the free surface displacement and velocity interferometrically, which were then related to interface stress. This technique was used to measure the tensile strength of a wide variety of metal/ceramic interfaces[22] and ceramic/ceramic interfaces[24] with the film thickness typically between 0.3-3 μm. More recently, Boustie *et al.*[25] used the laser spallation technique to test adhesion of some metal/metal film interfaces with film thicknessses of the order of tens of microns. In their tests, upper and lower laser intensity thresholds for spallation generation were determined experimentally and a traction range for debonding at the interface was determined numerically.

Past work has largely focused on evaluating film adhesion, with questions relating to optimal experiment design given less emphasis. The effect of laser fluence was investigated by Vossen,[12] Yang,[17] and Gupta *et al.*;[19] the effect of absorbing layer thickness was reported by Yang.[17] Although the effect of sharpness and shape of the stress pulse, film properties and film thickness were also studied by Yuan and Gupta,[21] their investigation was mainly based on numerical simulation. In order to get a better understanding of the mechanics of thin film spallation, we have judged it appropriate to systematically investigate the effects of film thickness, substrate thickness, and laser fluence. Here we report on a series of spallation experiments for Al thin films on both (100) Si and fused silica substrates of varying thickness. The results reveal important design parameters for laser spallation tests.

Laser Spallation Experiment

Experimental Procedure

Figure 1 describes the laser spallation experiment. The sample consists of a transparent confining layer, a thin energy absorbing layer, the substrate and the test film. An infrared, Nd:YAG pulse ($\lambda = 1064$ nm) with a variable energy content between 1 and 110 mJ is incident on a metallic absorbing layer sandwiched between the confining layer and the substrate. The shape of the laser pulse fits well to a Gaussian distribution of the form $I(t) = I_0 \exp(-t^2/T^2)$, where $I_0 = 18.9$ mJ/ns at full power and $T = 2.9$ ns. The energy-absorbing layer is chosen to be much thicker (typically $\sim$0.5 μm) than the critical penetration depth of laser light at this wavelength. Under this consideration, the laser energy is deposited at the interface of the confining layer and the energy-absorbing layer. The YAG pulse does not penetrate the substrate. A longitudinal stress wave of rise time comparable to that of the laser pulse is emitted from the absorbing layer. The wave that propagates towards the film/substrate interface is then reflected from the free surface and forms a tensile wave which then loads the test interface in tension.

The nominal diameter of the YAG laser beam is 3.5 mm. In order to increase the laser fluence, the laser beam is focused onto a 1–2 mm diameter spot on the energy-absorbing layer. The laser energy is increased until a longitudinal wave is generated with an amplitude sufficient to fail the film/substrate interface. Interferometric measurements of out-of-plane displacement are made at the surface of the test film. From displacement measurements at the free surface, the stress history at the interface is inferred using standard wave mechanics[26] and the maximum stress acting on the interface is calculated.

A detailed schematic of the Michaelson interferometer is shown in Fig. 2. A single, linearly polarized light beam of wavelength $\lambda_0 = 514.5$ nm from an argon laser is incident upon a beam splitting cube (BS). One beam is focused to a sharp point (less than 0.1 mm) on the test film using an objective lens, while the second beam is directed towards a stationary mirror (M2). The two beams are recombined in the beam splitter and then imaged onto the active area of photodiode detector. The signal from the detector is acquired using a digitizing oscilloscope.

Because the stress pulse in the experiment has a rise time of less than a few nanoseconds, fringes must be resolved with sub-nanosecond resolution. Such signals have been successfully measured in plate impact research,[27,28] shock wave studies[29] and previous spallation experiments.[19–24] An ultra-high speed photodector was selected with a rise time less than 300 ps. A high resolution LeCroy oscilloscope with a bandwidth of 1 GHz and a sample rate of 8G sample/s was used to record the interferometric fringes. Typical noise levels are less than 1% of a fringe.

Measuring Principles

Any movement of the sample surface causes a change in the signal frequency due to the Doppler effect. The Doppler frequency deviation for laser light of wavelength λ_0 reflected normally from a moving surface with velocity $V(t)$ is given by the Doppler shift equation as

$$\nu(t) = \frac{2V(t)}{\lambda_0}. \tag{1}$$

At the interferometer alignment of maximum sensitivity (the so-called $\pi/2$ point), the light intensity on the photodiode detector is related to the fringe count, $n(t)$, as

$$I(t) = \frac{I_{\max} + I_{\min}}{2} + \frac{I_{\max} - I_{\min}}{2} \sin(2\pi n(t) + \phi), \tag{2}$$

where $I_{\max}$ and $I_{\min}$ are the maximum and minimum intensities of the interference fringes and ϕ is the phase angle. The surface displacement is obtained in terms of the fringe count by integrating Eq (1):[29]

$$u(t) = \frac{\lambda_0 n(t)}{2}. \tag{3}$$

The fringe count is determined from the output of the photodiode detector (Eq (2)) and the displacement is calculated using Eq (3). One complete fringe shift corresponds to a displacement of $\lambda_0/2$ (257 nm). The resolution of this type of inteferometer is limited by the noise arising from fluctuations in the laser intensity and fluctuations in the environment (i.e., temperature). Once the free surface displacement is obtained from the interferometric measurements, the compressive stress propagating from absorbing layer towards the substrate is calculated using simple 1-D wave mechanics,

$$\sigma = -\frac{1}{2}(\rho c)_{substrate}\frac{\partial u}{\partial t}, \tag{4}$$

where ρ and c are the density and longitudinal wave speed of the substrate. Eq (4) assumes that the displacement amplitude of the wave in the substrate is half that of the wave at the free surface, as is justified provided the film is thin.

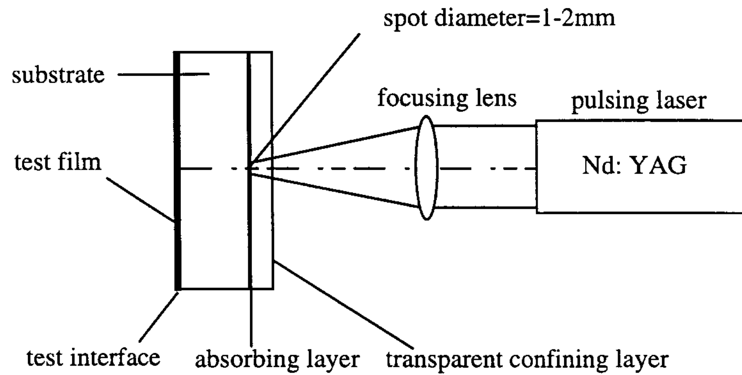

Fig. 1—Schematic of laser spallation technique: absorbing layer thicknesses are typically between $0.4 - 1.0$ μm, test film thicknesses are between $0.6 - 3.0$ μm and the substrate has a thickness between $400 - 6000$ μm

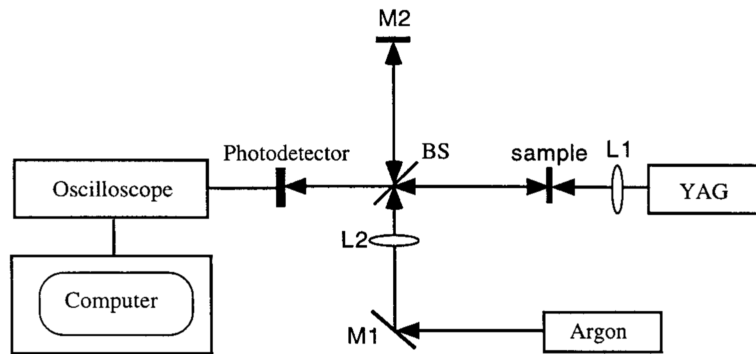

Fig. 2—Schematic of laser spallation experiment and interferometric displacement measurement

The stress acting on the interface is less than the stress of Eq (4) because the nearby free surface releases some of the stress. The relation can be calculated using elastic wave transmission and reflection coefficients. Here we make a simpler calculation, valid for small h, that the stress is ρh multiplied by the acceleration of the free surface. Thus the associated tensile stress that strikes the film/substrate interface is given by

$$\sigma_{interface} = -(\rho h)_{film} \frac{\partial^2 u}{\partial t^2}. \tag{5}$$

Eq (5) is equivalent to Newton's second law—the interface tensile stress is the mass density of the film times the outward acceleration of the center of mass of the film. This is the case regardless of the character of the propagation. That the measured surface displacement is a good approximation to the center of mass displacement follows from the known wave speeds in the film, the thickness of the film and the measured time scales in the wave.

Sample Fabrication

The thin film sample used for the spallation experiments is shown schematically in Fig. 3. For these experiments, an Al film was used for both the absorbing layer and the test film. The Al was deposited on either a fused silica or Si substrate.

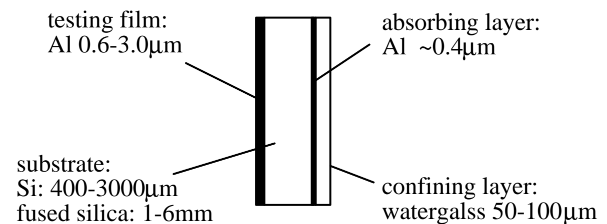

Fig. 3—Schematic of thin film sample for spallation experiment

For all the samples, waterglass was chosen as the confining material based on the work of previous researchers[22] and on an extensive test comparison of our own which concluded that waterglass provided consistent behavior and strong stress pulses with minimal expense.

For both fused silica and single side polished single crystal Si (100) substrates, aluminum films were plasma sputtered onto both sides using an ATC2000 sputtering system. The main chamber pressure was held at $4 - 8 \times 10^{-7}$ Torr and the sputtering rate was typically $1.5 - 2.0\, A°/s$. For the Si substrate samples, the Al layer on the rough side of the substrate was used as an absorbing layer, while the Al film on the

polished surface served as the test film. For all the samples, the absorbing layer was $0.4 - 1.0$ μm thick and the test film was $0.6 - 3$ μm thick. After deposition of the film, a thin layer of waterglass with thickness of $50-100$ μm was painted onto the back surface of the absorbing Al layer, as shown in Fig. 3.

Experimental Results

The thin film samples described above were tested using the experimental apparatus in Fig. 2. Prior to making any quantitative displacement measurements, a series of qualitative experiments were carried out to assess the influence of YAG laser fluence, thickness of the test film, and thickness of the substrate, on spallation and damage of the test film. Typical damage patterns on fused silica and Si substrate samples are shown in Figs. 4 and 5, respectively. Patterns like those of Figs. 4(a) and 5(a) typically appear at lower laser fluence ($\sim$0.07 J/mm^2) while patterns like those of Figs. 4(b) and 5(b) are representative of higher laser fluence ($\sim$ 0.14 J/mm^2). At higher laser fluence (Fig. 5(b)), there is a large amount of substrate damage ($\sim$60 μm deep) in the Si due to cleavage under the action of the tensile wave. Since the adhesion between the film and substrate is of primary interest, substrate cleavage is not desired. In the fused silica substrate samples, however, no substrate damage was observed. This suggests that fused silica may be a more ideal substrate material for studying the mechanics of the spallation test.

The effects of film and substrate thickness are summarized in Table 1. For both fused silica and Si substrate samples, greater amounts of film damage occurred at higher YAG laser fluence. Moreover, the thicker the test film and the thinner the substrate, the greater the extent of the damage.

Quantitative measurements of the displacement, substrate stress and interface stress were obtained using a Michaelson interferometer as shown in Fig. 2. A typical interferometric signal measured for an Al test film on a Si substrate is shown in Fig. 6(a). Using Eqs (2) and (3), the displacement profile of the film free surface (Fig. 6(b)) is determined from the fringe data (Fig. 6(a)). As discussed in the section on measuring principles above, the compressive substrate stress (Fig. 6(c)) and the stress at the test film interface after reflecting from the free surface (Fig. 6(d)) are calculated from Eqs (4) and (5), respectively.

In the data for Si samples shown in Fig. 6, five fringes developed within 15 ns, corresponding to a maximum displacement of 1400 nm. The maximum compressive substrate stress of 1.7 GPa was achieved shortly after the wave arrival

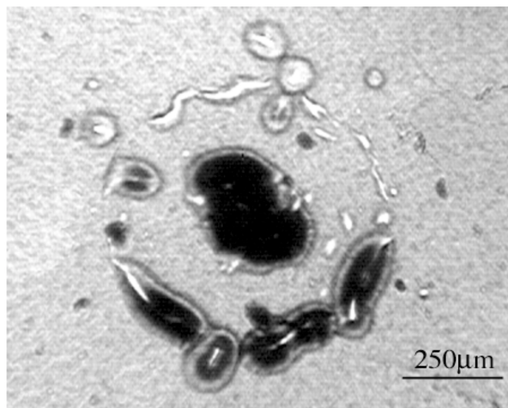

(a)

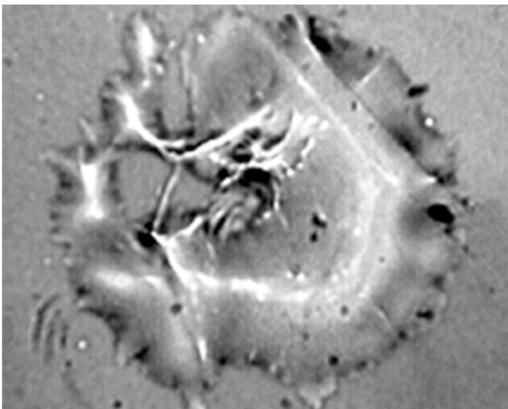

(b)

Fig. 4—Typical damage patterns on 3063 μm thick fused silica substrate sample: (a) lower laser fluence ($\sim$0.07 J/mm^2), light area is the intact film, dark area is the lifted film; (b) higher laser fluence ($\sim$0.14 J/mm^2), central region is the lifted film from the substrate. The diameter of the laser spot is about 1 mm

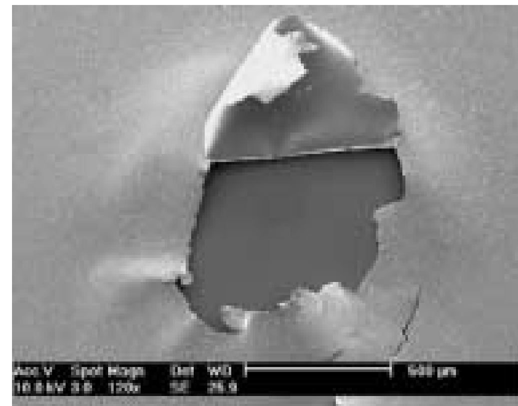

(a)

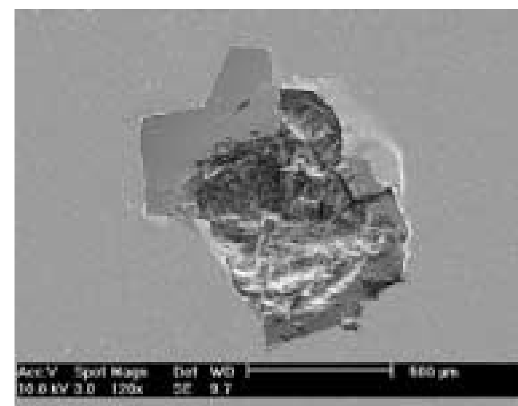

(b)

Fig. 5—Typical damage patterns on 600 μm thick Si substrate sample (a) lower laser fluence ($\sim$0.07 J/mm^2); (b) higher laser fluence ($\sim$0.14 J/mm^2)

TABLE 1—EFFECT OF Al FILM/Si SUBSTRATE THICKNESS ON SPALLATION

Test Film	Substrate Thickness (μm)			
Thickness (μm)	400	500	700	3000
0.6	Yes	Yes	No	No
1.0	Yes	Yes	Yes	No
1.5	Yes	Yes	Yes	No
3.0				Yes

NOTE: Yes means some spallation is observed; No means no spallation at all.

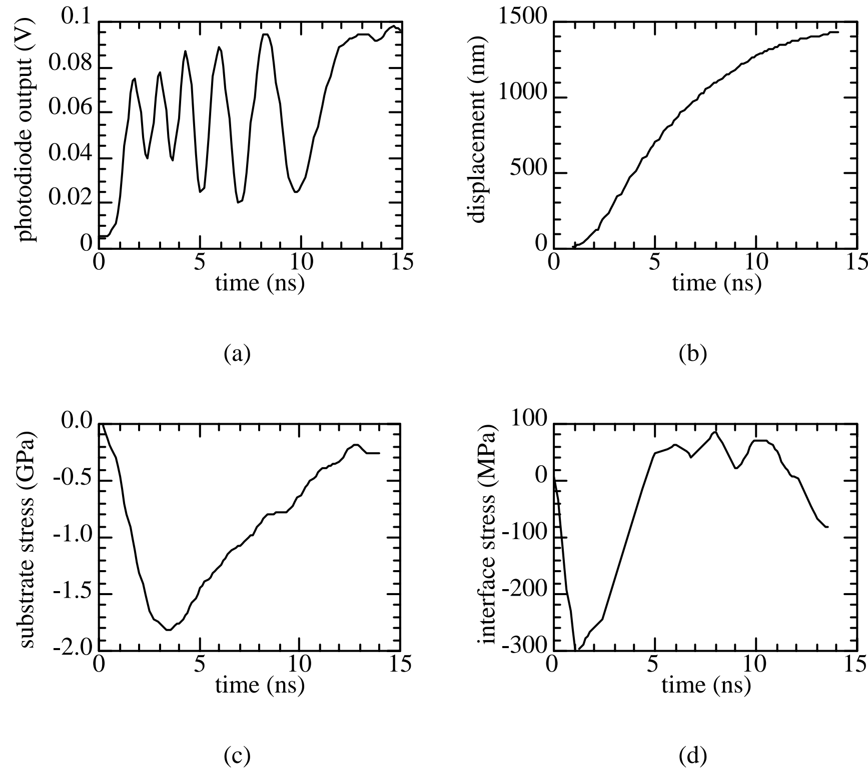

Fig. 6—A typical data processing cycle for a 600 μm thick Si substrate sample: (a) interferometric fringe pattern; (b) displacement profile; (c) substrate stress profile; (d) interface stress profile

and the maximum tensile interface stress of 60 MPa occurred slightly later. The long fall time in Fig. 6(c) leads to only modest tensile loading of the test film interface. Despite the differences between the laser pulses, thicknesses of the film, substrate and confining layer, the magnitudes of the stress in Si substrate in current work falls in the same range as those reported by Yuan and Gupta.[21]

Interferometric data are shown in Figs. 7 and 8 for fused silica substrates of thicknesses 1531 and 3063 μm. Figs. 7(a) and 8(a) show the raw fringe data. The other figures show the results from processing that data, the associated displacements and stresses. In both cases the fringe data is significantly different from that of the Si substrate. The fringes develop over 20 to 30 ns in fused silica, whereas in Si the full waveform was confined to a duration of about 10 ns comparable to the duration of the YAG pulse. In Si the spacings between successive fringes grow with time; in fused silica the fringes become more tightly spaced. Possibly most telling is the occurrence (marked by an arrow in Fig. 8(a)) of a turning point, where the material velocity changes direction in the middle of a fringe. That there is a turning point here (and a sudden zeroing of material velocity in the 1531 μm sample at 25 ns) is supported by theoretical considerations. Fused silica has significant nonlinear elastic properties, softening at compressive strains up to 5% and stiffening at higher strains. This behavior is well documented by studies of shocks from the impact of flyer plates.[29] The nonlinear evolution of a nominally Gaussian compressive pulse, as we expect our initial wave to be, can be described qualitatively. The low compressive stresses at the front of the pulse travel most quickly. The peak stresses, initially a few nanoseconds behind the front of the pulse, are retarded relative to the front of the pulse. The rising part of the compression pulse thus evolves into a linear ramp, a classic acceleration wave. This ramp is precisely what is seen in Figs 7(c) and 8(c). The slope of that ramp (in units of stress per {time/thickness}) is a material parameter and is the same as that reported by Barker and Hollenbach.[29]

The falling part of the stress pulse evolves in a very different manner. The tail of the initial pulse propagates more quickly than does the peak. It overtakes the peak in a time which may be calculated using the material properties apparent in the slope of the ramp. A discontinuity in stress

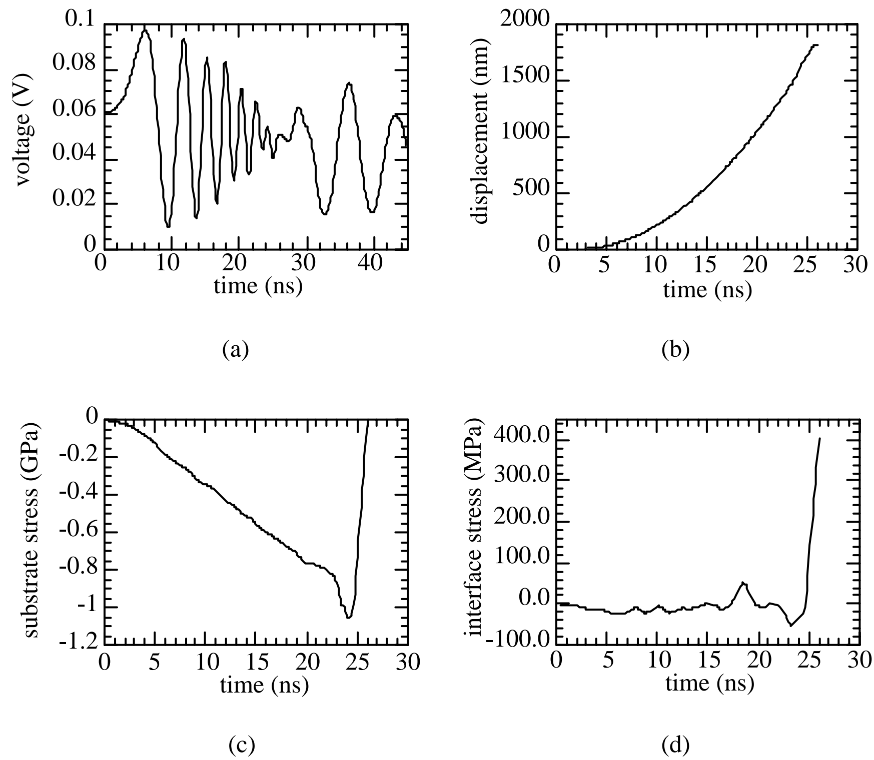

Fig. 7—Typical data profile for a fused silica (1531 μm thick) substrate sample: (a) interferometric fringe pattern; (b) displacement profile; (c) substrate stress profile; (d) interface stress profile

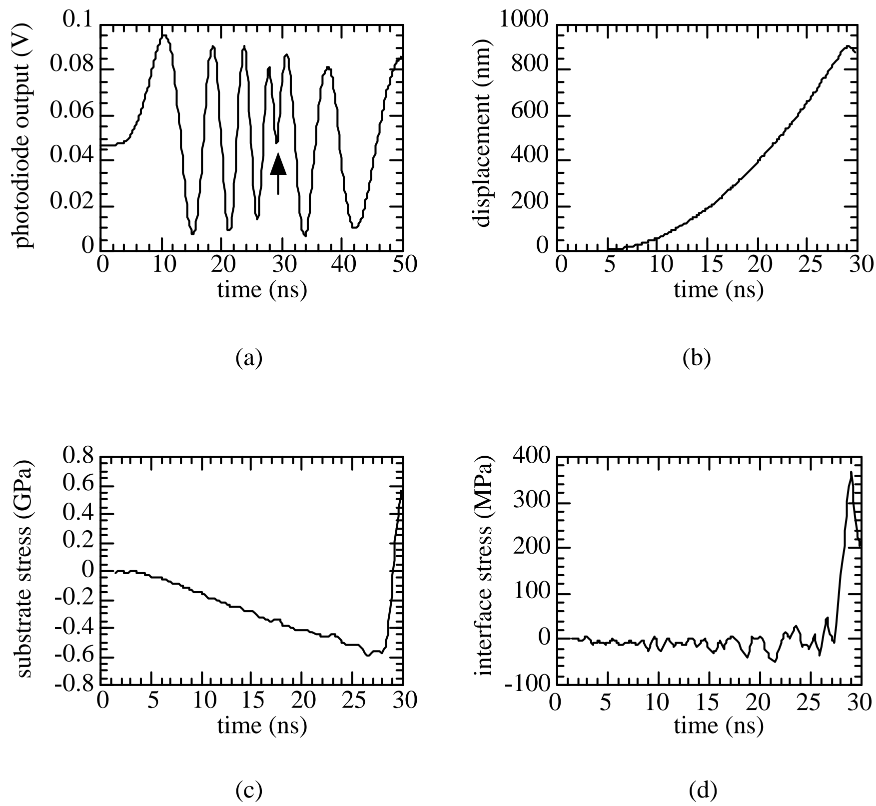

Fig. 8—Typical data profile for a fused silica (3063 μm thick) substrate sample: (a) interferometric fringe pattern, arrow points to turning point; (b) displacement profile; (c) substrate stress profile; (d) interface stress profile

(and therefore also in material velocity) develops when the tail overtakes the peak. The theory of the development and subsequent evolution of such "weak shocks" may be found in standard references.[30–32] That sufficient time has occurred in the present case for a decompression shock to develop is evident. After traveling through the substrate, the rising front of the pulse has stretched from about 2.9 ns to 20 or 30 ns. The falling rear of the pulse has therefore compressed by the same amount; an initial fall time of a few nanoseconds has therefore been reduced to zero, and this occurs long before the pulse arrives at the test film.

The experimental picture is complicated somewhat by the presence of a tensile wave, reflected from the back of the confining layer. The thickness and the surface properties of that confining layer are not well controlled. Assuming a plausible longitudinal wavespeed in the confining layer, the original compressive pulse is followed, about 30 ns later, by a tensile pulse of comparable magnitude. Being tensile, it propagates faster than the peak compressive stress, and faster than the low stress tail of the main pulse. It therefore eventually overtakes the compressive pulse. In Fig. 8 we see that the shock is followed by a regime in which the velocity has changed sign; here we conclude that the tensile pulse has overtaken the compression pulse. In Fig. 7, the shock is immediately followed by a regime of small material velocity and 10 ns later by a regime of larger velocity. Here we conclude that the tensile pulse has not yet overtaken the main compression pulse. The decompression shock is especially beneficial for tensile thin surface film test, where the optimal compressive pulse ought to have a rapid fall time.[23] Linear dissipative mechanisms govern the thickness of shocks.

Using these data acquisition and processing procedures, a large number of tests were performed on both Si and fused silica samples. The effects of laser power, substrate thickness, and film thickness were investigated and the results summarized below.

Parametric Studies

Effect of Laser Fluence

The effect of laser fluence was studied on a sample with a test film thickness of 1.1 μm, fused silica substrate thickness of 3063 μm and absorbing layer thickness of 0.4 μm. The YAG laser fluence was stepped from 0.056 to 0.14 J/mm^2 as the YAG spot was moved to different positions on the sample. Figure 9 shows the development of stress with increasing laser power. As laser fluence increases, the maximum compressive substrate stress also increases. At 0.056 J/mm^2 laser fluence, the maximum substrate stress of 0.28 GPa is achieved in a rise time of 18 ns; while for 0.14 J/mm^2 laser fluence a maximum substrate stress of 0.6 GPa is obtained in 28.5 ns. The higher maximum stress always occurs at later times and is approximately proportional to the laser fluence. The shock profiles in Fig. 9 are consistent with the nonlinear behavior of fused silica. The slope of the stress ramps agrees with Barker's material parameters.[31] From these stress profiles, an effective wavespeed can be extracted as a function of stress. The higher compressive stresses arrive later because higher compression means slower waves.

The corresponding tensile interface stress can be estimated from Fig. 9 as described previously. The maximum interface stresses are 200, 100, 350 and 400 MPa, for 0.056, 0.084, 0.112, and 0.14 J/mm^2 laser fluence, respectively. These

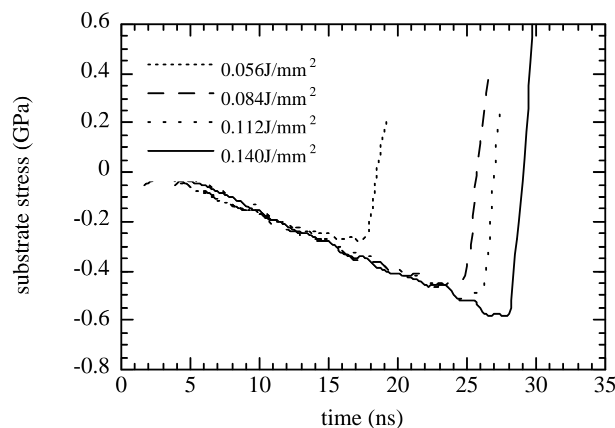

Fig. 9—Effect of laser fluence on fused silica (3063 μm) substrate sample: test film thickness: 1.1 μm, absorbing layer thickness: 0.4 μm

numbers are obtained by numerical differentiation of the data of Fig. 9 and are somewhat imprecise. Overall, the maximum interface stress increases with increasing laser fluence.

The effect of laser fluence was also studied on a 600 μm thick Si wafer with a 1.1 μm thick test film and 0.4 μm absorbing layer. As YAG laser fluence increased from 0.056 to 0.14 J/mm^2, the maximum compressive substrate stress increased from 0.7 to 2.3 GPa, and in all cases occurred at approximately the same time after the wave's initial arrival, about 3.5 ns, comparable to the rise time of the laser pulse. The corresponding maximum tensile interface stress also increased from 60 to 100 MPa.

Although the maximum substrate stress and maximum interface stress increase as laser fluence increases for both fused silica and Si substrate samples, the data are quite different for the two kinds of samples. The maximum substrate stress and interface stress for the Si samples were achieved in a very short time, usually within 5 ns after the wave arrival. But for the fused silica substrate, the rise of the maximum substrate stress and interface stress was slower (from 15 to 30 ns). These differences are due to the development of a decompression shock in the fused silica substrate. In addition, the shock is responsible for the much greater interface stress in fused silica samples than in the Si samples.

Effect of Film Thickness

The effect of test film thickness was studied for 3063 μm thick fused silica substrate samples. Three film thicknesses, 1.1, 1.45, and 1.90 μm, were tested at full laser power. The absorbing layer thicknesses varied between 0.4 and 0.54 μm for these samples. Previous experiments by Yang[17] indicated that small variations in absorbing layer thickness have little effect on the generated stress. The results for these tests are summarized in Table 2. The maximum interface stress was found to be greater for thicker films. The large increase in interface stress for the 1.9 μm film, however, may be due to imperfect stress pulse generation or imprecision in the measurement. A small increase in the maximum substrate stress is also measured for increasing film thickness. This anomalous increase is possibly due to effects of nonzero test film thickness.

TABLE 2—EFFECT OF TEST FILM THICKNESS ON $\sigma_{substrate}^{max}$ and $\sigma_{interface}^{max}$ FOR FUSED SILICA SAMPLES

Film thickness (μm)	1.1	1.45	1.9
$\sigma_{substrate}^{max}$ (GPa)	−0.6	−0.7	−0.8
$\sigma_{interface}^{max}$ (MPa)	400	600	1000

Effect of Substrate Thickness

The influence of substrate thickness was investigated for both fused silica and Si substrate samples with a 1.1 μm thick test film and 0.4 μm thick absorbing layer. The resulting maximum substrate stress and maximum interface stress values are summarized in Table 3 for three thicknesses of fused silica (1531, 3063, and 6125 μm) and in Table 4 for three thicknesses of Si (400, 600, and 3000 μm). The interferometric data are similar to Fig. 6 for each thickness of Si. Fringe patterns for 6125 μm thick fused silica are similar to Fig. 8. A decompression shock was observed for all three thicknesses of the fused silica. For both types of samples, the maximum substrate stress and maximum interface stress were found to be less for greater substrate thickness.

After the initial reports by Gupta *et al.*, the issue of geometric attenuation, and the related transition of the initial planar wave front to a spherical wave, was extensively discussed in the literature.[33–35] The attenuation of the maximum substrate stress and maximum interface stress is geometric and due to the finite spatial width of the YAG source. Intrinsic attenuation is known to be weak in these materials.[36] The issue appears to have been settled by numerical calculations in the report by Lev and Argon[34] in which it was concluded that the front remains essentially planar for a distance comparable to two or three times the radius of the laser spot. This conclusion was based on numerical observations of diminishment of peak stress amplitude at such distances. This conservative estimate may be compared with the standard acoustician's rule, that the near field of a planar acoustic source of diameter D extends a distance $D^2/4\lambda_e$.[37] Even if one takes the ultrasonic elastic wavelength λ_e to be as much as 60 microns—corresponding to the length of the longitudinal disturbance generated by a 10 ns laser pulse—a 1 mm diameter spot will generate a wave which remains approximately plane over a distance of 4 mm. For this reason, we anticipate only modest losses due to geometric attenuation for substrates less than 4 mm thick. In addition, our use of laser interferometry to directly measure the surface displacement of the film during spallation eliminates the need for detailed stress calculations. Interface stress is the mass density of the film times the outward acceleration of the center of mass of the film, regardless of the 1-D or 2-D character of the propagation. For the present discussion, the effect of the substrate thickness is estimated analytically by considering a circular region of diameter D, as shown in Fig. 10.

Previous theoretical analysis of the wave generation mechanism[38] indicates that the stress pulse in the source region generated by current YAG laser has the same shape as the laser pulse and can be expressed using a Gaussian distribution:

$$\sigma(t) = \sigma_{max} \exp\left(-\frac{t^2}{T^2}\right), \tag{6}$$

where σ_{max} is the maximum compressive stress and $T = 2.9$ ns. Thus, using Huygen's principle, the stress wave in an isotropic linear medium on axis at distance r from the source can be approximated by an integral over the entire source region, i.e.,

$$\sigma(r,t;D) = \frac{A}{D^2}\int_0^{2\pi}\int_0^{D/2} \frac{1}{\sqrt{r^2+x^2}} \exp\left(-\frac{\left(t-\sqrt{r^2+x^2}/c\right)^2}{T^2}\right) x\,dx\,d\theta. \tag{7}$$

The stress at the test film interface is proportional to the time derivative of (7), i.e.,

$$\sigma_{interface}(r,t;D) = \frac{B}{D^2}\int_0^{2\pi}\int_0^{D/2} \frac{t-\sqrt{r^2+x^2}/c}{\sqrt{r^2+x^2}} \exp\left(-\frac{\left(t-\sqrt{r^2+x^2}/c\right)^2}{T^2}\right) x\,dx\,d\theta, \tag{8}$$

where A and B are constants. These integrals can be evaluated analytically,

TABLE 3—EFFECT OF SUBSTRATE THICKNESS ON Si SUBSTRATE SAMPLES

Substrate thickness (μm)	400	600	3000
$\sigma_{substrate}^{max}$ (GPa)	−1.7	−1.4	−0.55
$\sigma_{interface}^{max}$ (MPa)	100	90	75

TABLE 4—EFFECT OF SUBSTRATE THICKNESS ON FUSED SILICA SAMPLES

Substrate thickness (μm)	1531	3063	6125
$\sigma_{substrate}^{max}$ (GPa)	−1.2	−0.5	−0.3
$\sigma_{interface}^{max}$ (MPa)	370	350	50

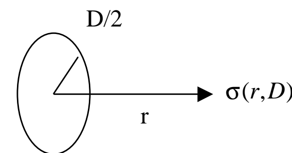

Fig. 10—Stress generated by a finite sized pancake YAG source

$$\sigma(r, t; D) \propto \frac{1}{D^2}\left[erf\left(\frac{\sqrt{r^2 + D^2/4}/c - t}{T}\right) - erf\left(\frac{r/c - t}{T}\right)\right] \quad (9)$$

and

$$\sigma(r, t; D)_{interface} \propto \frac{1}{D^2}\left[\exp\left(-\frac{\left(\sqrt{r^2 + D^2/4}/c - t\right)^2}{T^2}\right) - \exp\left(-\frac{(r/c - t)^2}{T^2}\right)\right]. \quad (10)$$

The relative maximum stress in the substrate and maximum stress at the interface were evaluated for different source size D at different distances r and are plotted in Figs. 11 and 12.

At fixed pulsed laser energy, the larger the source diameter, the lower the maximum substrate and interface stress. For the same source diameter, greater attenuation occurs at longer distances. The diameter of the laser spot in the current experiment is about 1 mm. Based on the $D = 1$ mm curves in Figs. 11 and 12, the maximum substrate stress begins to attenuate (as quantified by a 10% drop) after about 2 mm and the maximum interface stress begins to attenuate after 3.5 mm. The maximum substrate stress attenuates faster than the maximum interface stress. These features of the simplified theoretical analysis are consistent with the observations of the effect of substrate thickness reported in Tables 3 and 4.

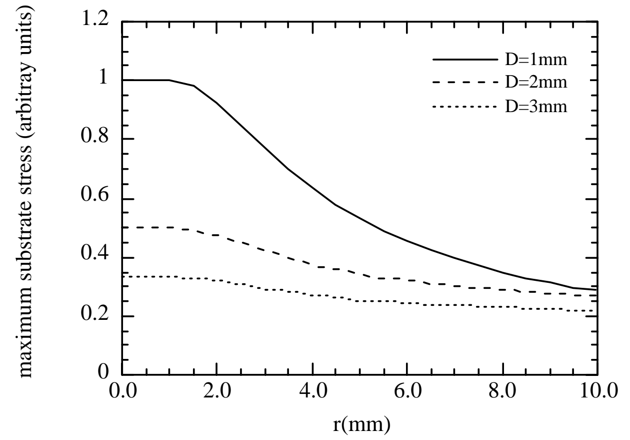

Fig. 11—Attenuation of maximum substrate stress with regard to distance and source diameter. Data were normalized by the maximum stress for $D = 1$ mm at $r = 0$

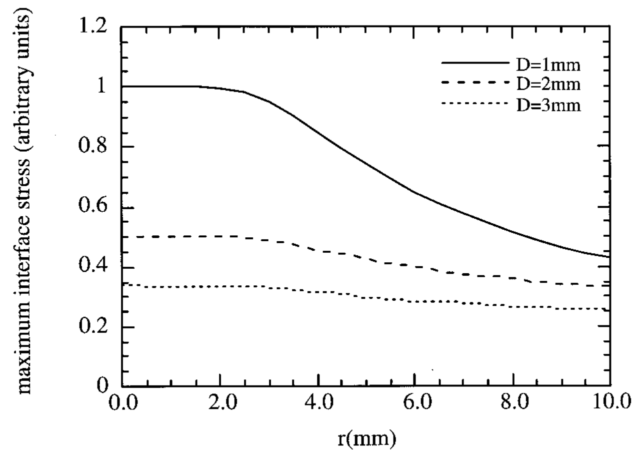

Fig. 12—Attenuation of maximum interface stress with regard to distance and source diameter. Data were normalized by the maximum stress for $D = 1$ mm at $r = 0$

Conclusions

For both fused silica and Si substrate samples, the maximum stress in the substrate and the maximum stress at the interface increased with increasing YAG laser fluence. For fused silica substrate samples with test film thickness in the range of 1.1 to 1.9 μm, the maximum interface stress also increased with increasing film thickness. Hence, thicker films lead to higher interface stress and fail more easily. For both types of samples, the maximum substrate stress and maximum interface stress decreased with increasing substrate thickness due to the finite diameter of the YAG source and geometric attenuation. Analytical estimates show that the stress level could be enhanced by reducing either the YAG spot size or the substrate thickness. In practical experiments, several factors including YAG spot size, film thickness and substrate thickness must be coordinated.

Qualitative observations of damage revealed both substrate and film failure in Si substrate samples but only film failure in fused silica substrate samples. Quantitative interferometric measurements confirmed the difference in the stress development for the two kinds of samples. In fused silica substrates, the compressive pulse evolved into a decompression shock. The existence of a shock created a large stress at the film interface, promoting failure. The development of the shock is due to the nonlinear elastic properties of fused silica.[29] This shock mechanism is advantageous in the design of laser spallation tests of thin film interface adhesion. Moreover, fused silica is an ideal material for studying the mechanics of the spallation test in that it is intrinsically strong and no substrate damage occurs before the interfacial failure. Although shock development in fused silica was demonstrated in the 1970s by Barker and Hollenbach using a gas-gun facility, the usefulness of such shocks in applications to laser spallation has not been reported.

Acknowledgments

The authors gratefully acknowledge the support of the National Science Foundation (CMS-99-88127) and the University of Illinois Research Board. We would also like to acknowledge the use of the Frederick Seitz Materials Research Lab facilities at the University of Illinois.

References

1. Evans, A. and Hutchinson, J., "The Thermomechanical Integrity of Thin Films and Multilayers," Acta. Metall. Mater., **43***, 2507–2530 (1995).*

2. Heavens, O.S., "Some Factors Influencing the Adhesion of Films Produced by Vacuum Evaporation," J. Phys. Radium, **11***, 355–360 (1950).*

3. Weaver, C., "Adhesion of Thin Films," J. Vac. Sci. Technol., **12**, 18–25 (1975).

4. Laugier, M., "The Development of the Scratch Technique for the Determination of the Adhesion of Coatings," Thin Solid Films, **76** (3), 289–294 (1981).

5. Hull, T.R., Colligon, J.S., and Hill, A.E., "Measurement of Thin Film Adhesion," Vacuum, **37**, 327–330 (1987).

6. Strong, J., "On the Cleaning of Surfaces," Rev. Sci. Instrum., **6**, 97–98 (1935).

7. Jacobsson, R., "Measurement of Adhesion of Thin Films," Thin Solid Films, **34**, 191–199 (1976).

8. Gent, A.N. and Lewandowski, L.H., "Blow-off Pressures for Adhering Layers, J. Appl. Polym. Sci., **33**, 1567–1577 (1987).

9. Chu, Y.Z., Jeong, H.S., White, R.C., and Durning, C.J., "Characterization of Adhesion in Thin-film Materials by the Blister Test," Mat. Res. Soc. Symp. Proc., **276**, 209–220 (1992).

10. Kriese, M.D., Gerberich, W.W., and Moody, N.R., "Quantitative Adhesion Measures of Multiplayer Films: Part I. Indentation Mechanics," J. Mater. Res., **14** (7), 3007–3018 (1999).

11. Kriese, M.D., Gerberich, W.W., and Moody, N.R., "Quantitative Adhesion Measures of Multiplayer Films: Part II. Indentation of W/Cu, W/W, Cr/W," J. Mater. Res., **14** (7), 3019–3026 (1999).

12. Thouless, M.D., "Fracture Mechanics for Thin Film Adhesion," IBM J. Res. Develop. **38**, 367–377 (1994).

13. Vossen, J.L., in "Adhesion Measurement of Thin Films, Thick Films and Bulk Coatings," ASTM STP640, 122–133 (1978).

14. Ready, J.F., "Effects Due to Absorption of Laser Radiation," J. Appl. Phys., **36**, 462–468 (1965).

15. Anderholm, N.C., "Laser Generated Stress Waves." Appl. Phys. Lett., **16** (3), 113–115 (1970).

16. Peercy, P.S., Jones, E.D., Bushnell, J.C., and Gobeli, G.W., "Ultrafast Rise Time Laser Induced Stress Waves," Appl. Phys. Lett., **16**, 120–122 (1970).

17. Yang, L.C., "Stress Waves Generated in Thin Metallic Films By a Q-switched Ruby Laser," J. Appl. Phys., **45** (6), 2602–2608 (1974).

18. Fox, J.A., "Effect of Pulse Shaping on Laser-induced Spallation," Appl. Phys. Lett., **24**, 340–343 (1974).

19. Gupta, V., Argon, A.S., Cornie, J.A., and Parks, D.M., "Measurement of Interface Strength by Laser Pulse-induced Spallation," Mater. Sci. Eng., **A126**, 105–117 (1990).

20. Gupta, V., Argon, A.S., Parks, D.M. and Cornie, J.A., "Measurement of Interface Strength by a Laser Spallation Technique," J. Mech. Phys. Solids, **40**, 141–180 (1992).

21. Yuan, J. and Gupta, V., "Measurement of Interface Strength by the Modified Laser Spallation Technique. I. Experiment and Simulation of the Spallation Process," J. Appl. Phys., **74**, 388–2396 (1993).

22. Gupta, V. and Yuan, J., "Measurement of Interface Strength by the Modified Laser Spallation Technique. II. Applications to Metal/Ceramic Interfaces," J. Appl. Phys., **74**, 2397–2404 (1993).

23. Yuan, J., Gupta, V., and Pronin, A., "Measurement of Interface Strength by the Modified Laser Spallation Technique. III. Experimental Optimization of the Stress Pulse," J. Appl. Phys., **74**, 2405–2410 (1993).

24. Gupta, V., Yuan, J., and Pronin, A., "Recent Developments in the Laser Spallation Technique to Measure the Interface Strength and Its Relationship to Interface Toughness with Applications to Metal/Ceramic, Ceramic/Ceramic and Ceramic/Polymer Interfaces," J. Adhesion Sci. Technol., **8**, 713–747 (1994).

25. Boustie, M., Auronz, E., Romain, J.P., Bertoli, A., and Manesse, D., "Determination of the Bond Strength of Some Microns Coatings Using the Laser Shock Technique," Eur. Phys. J. **AP5**, 149–153 (1999).

26. Miklowitz, J., "Elastic Waves and Waveguides," North Holland (1978).

27. Zhou, M. and Clifton, R.J., "Dynamic Ductile Rupture under Conditions of Plane Strain," J. Appl. Phys., **74**, 2405–2410 (1997).

28. Raiser, G.F., Wise, J.L., Clifton, R.J., Grady, D.E., and Cox, D.E., "Plate Impact Response of Ceramics and Glasses," J. Appl. Phys., **75**, 3862–3869 (1994).

29. Barker, L.M. and Hollenbach, R.E., "Shock Wave Studies of PMMA, Fused Silica and Sappire," J. Appl. Phys., **41**, 4208–4226 (1970).

30. Nunziato, J.W., Walsh, E.K., Schuler. K.W., and Barker, L.M., "Wave Propagation in Nonlinear Viscoelastic Solids," in Mechanics of Solids, C. Truesdell, ed., Springer Verlag, **IV**, 1–108 (1984).

31. Thurston, R.N., "Waves in Solids," in Mechanics of Solids, C. Tresdell, ed., Springer Verlag, **IV**, 109–308 (1984).

32. Pierce, A., Acoustics, McGraw-Hill (1981).

33. Nutt, G.L. and King, W.E., "Comments on the Bond Strength Measurement of Gupta and Co-workers," Materials Science and Engineering, **A159**, 135–142 (1992).

34. Lev, L.C. and Argon, A.S., "Spallation of Thin Elastic Coating from Elastic Substrates by Laser Induced Pressure Pulses," J. Appl. Phys., **80**, 529–542 (1996).

35. Argon, A.S., Cornie, J.A., Gupta, V., Lev, L., and Parks, D.M., "Response to the Comments of Nutt and King on the Bond Strength Measurements of Gupta et al.," Materials Science and Engineering, **A37**, 224–228 (1997).

36. Lamb, J., Redwood, M., and Shteinshleifer, Z., "Absorption of Compressional Waves in Solids from 100 to 1000 MC/Sec," Physical Review Letters, **3** (1), 28–29 (1959).

37. Kinsler L.E., Frey, A.R., Coppens, A.B., and Sanders, J.V., Fundamentals of Acoustics, John Wiley & Sons, New York (1980).

38. Wang, J., Sottos, N. R., and Weaver, R. L., "Laser Induced Thin Film Spallation," TAM Report No. 944, UILU-ENG-2000-6019, Theoretical and Applied Mechanics Department, University of Illinois at Urbana-Champaign (2000).